

## Powder Conductivities of Three Electrides

Kevin J. Moeggenborg, John Papaioannou,<sup>†</sup> and James L. Dye\*

Department of Chemistry and Center for Fundamental Materials Research, Michigan State University, East Lansing, Michigan 48824

Received December 20, 1990. Revised Manuscript Received March 13, 1991

Electrical measurements on electride samples show a wide range of behavior in this novel class of compounds.  $K^+(C222)e^-$ , in which C222 represents cryptand [2.2.2], is highly conductive. Most of the measured resistance and the nonohmic behavior observed in two-probe measurements with inert electrodes result from either a Schottky barrier or a resistive barrier at the sample-electrode interface. By use of potassium metal on the electrodes, this effect was nearly eliminated, and the electrode impedance decreased by 4 orders of magnitude. An upper limit of 0.2  $\Omega$  cm for the resistivity of  $K^+(C222)e^-$  at 130 K was obtained through the use of the van der Pauw technique on pellets and apparent bandgaps of 0.086 and 0.055 above and below 135 K, respectively, were determined. The residual resistivity could be due to activated transport of electrons across grain boundaries. In contrast to the high electronic conductivity of  $K^+(C222)e^-$ , the electrides  $Cs^+(15C5)_2e^-$  and  $Cs^+(18C6)_2e^-$ , in which the cation is present in a crown ether sandwich, exhibit very low electronic conductivities but appear to be the first examples of ionically conductive electrides. The mechanism may involve release of the cesium cation from its crown ether cage, coupled with its reduction to  $Cs^0$  by a trapped electron. Ionic conductivity could then result from the transfer of  $Cs^+$  between anionic sites in the lattice. The activation energies for ionic conductivity are about 1.1 eV for  $Cs^+(18C6)_2e^-$  and 0.6 eV for  $Cs^+(15C5)_2e^-$ . The presence of small amounts of excess cesium metal in  $Cs^+(18C6)_2e^-$ , to provide a mixed ceside-electride, leads to greatly increased electronic conductivity and is probably the origin of semiconductor behavior previously seen for this compound.

### Introduction

Alkalides and electrides are two novel classes of crystalline ionic salts whose cations are complexed alkali-metal cations and whose anions are either alkali-metal anions (alkalides) or trapped electrons (electrides). More than 40 of these compounds have been synthesized and characterized as described in three review articles.<sup>1-3</sup> Optical, NMR, and EPR spectra, magnetic susceptibilities, and pressed powder dc conductivities have been studied, and the crystal structures of 30 alkalides and 4 electrides have been determined. The unusual nature of the anions in these compounds makes their electrical properties of interest. In particular, since electrides contain complexed cations and rather weakly bound electrons, they could behave as either semiconductors or metals.

Early dc conductivity experiments on pressed powder samples of  $Na^+(\text{cryptand}[2.2.2]Na^-)$  [abbreviated  $Na^+(C222)Na^-$ ] indicated that it was a semiconductor with an apparent bandgap of 2.4 eV (activation energy of 1.2 eV).<sup>1,4,5</sup> Later electrical studies performed on single crystals of  $Na^+(C222)Na^-$  confirmed the 2.4-eV bandgap and showed the alkalide to be an intrinsic semiconductor.<sup>6</sup> At higher temperatures, cationic conductivity with an activation energy of 1.6 eV was also observed in single crystals of  $Na^+(C222)Na^-$ . Temperature-dependent dc conductivity studies of pressed powder samples of other alkalides and electrides also showed semiconductor-like behavior with apparent bandgaps of 0.6-2.4 eV.<sup>1,2,7,8</sup> The tendency of these compounds to decompose and their reactivity toward air and moisture have made detailed electrical studies difficult. All operations with alkalides and electrides must be performed under inert atmosphere or vacuum and at temperatures typically below -40 °C. In addition, the synthesis of alkalide salts usually produces compounds that contain defect-trapped electrons. These electrons are trapped in potential wells that are shallow compared with electron binding to  $M^-$  and thus dominate the conductivity, leading to low apparent bandgaps. One of the few exceptions to this behavior is  $Na^+(C222)Na^-$ ,

which can be synthesized nearly free of defect electrons as indicated by EPR spectroscopy. We must also assume that alkalide impurities can exist in electrides and that this may also affect their conductivity.

The inability to grow large single crystals and the difficulty in attaching wires to the crystals has so far restricted the use of single-crystal conductivity methods to  $Na^+(C222)Na^-$ , for which it was possible to measure the transverse conductivity of platelike single crystals.<sup>6</sup> As a result of these difficulties, all other previous electrical studies of these compounds utilized dc conductivity methods and pressed powder samples. In the present work, in addition to dc conductivities of pressed powders, impedance spectroscopy and four-probe ac conductivity measurements were made on pressed powders and pellets. We report here studies of three electrides for which crystal structures have been determined,  $K^+(C222)e^-$ ,  $Cs^+(15\text{-crown-5})_2e^-$ , and  $Cs^+(18\text{-crown-6})_2e^-$ . The latter two compounds are abbreviated  $Cs^+(15C5)_2e^-$  and  $Cs^+(18C6)_2e^-$ , respectively.

### Experimental Section

The pure electride samples were synthesized as previously described,<sup>7,9,10</sup> except that a slight excess (5-25%) of complexant was used in each case to minimize contamination by  $M^-$ . Alkalide-doped samples of  $Cs^+(18C6)_2e^-$  were prepared by two methods: method A was identical with that used in the synthesis of the pure compound except that no excess complexant was used;

- (1) Dye, J. L. *Prog. Inorg. Chem.* **1984**, *32*, 327-441.
- (2) Dye, J. L.; DeBacker, M. G. *Annu. Rev. Phys. Chem.* **1987**, *38*, 271-301.
- (3) Dye, J. L. *Science* **1990**, *247*, 663-668.
- (4) Dye, J. L.; Ceraso, J. M.; Lok, M. T.; Barnett, B. L.; Tehan, F. J. *J. Am. Chem. Soc.* **1974**, *96*, 608-609.
- (5) Dye, J. L. *Angew. Chem.* **1979**, *18*, 587-598.
- (6) Papaioannou, J.; Jaenicke, S.; Dye, J. L. *J. Solid State Chem.* **1987**, *67*, 122-130.
- (7) Ellaboudy, A.; Dye, J. L.; Smith, P. B. *J. Am. Chem. Soc.* **1983**, *105*, 6490-6491.
- (8) Dye, J. L.; Ellaboudy, A. *Chem. Brit.* **1984**, *20*, 210-215.
- (9) Van Eck, B.; Le, L. D.; Issa, D.; Dye, J. L. *Inorg. Chem.* **1982**, *21*, 1966-1970.
- (10) Dye, J. L. *J. Phys. Chem.* **1984**, *88*, 3842-3846.

<sup>†</sup>Department of Chemistry, University of Athens, Greece.

\*To whom correspondence should be addressed.

in method B, pure samples of  $\text{Cs}^+(18\text{C}6)_2\text{e}^-$  were mixed with small amounts of  $\text{Cs}^+(18\text{C}6)_2\text{Cs}^-$ , in the case of ceside doping, or with  $\text{Cs}^+(18\text{C}6)_2\text{Na}^-$ , in the case of sodide doping. The two compounds were placed in a crystallization cell in a nitrogen-filled glovebag at liquid nitrogen temperatures. Roughly 10% of the sample was alkalide, although thermal instabilities prevented the use of weighed amounts of the two compounds. The mixture was then dissolved in dimethyl ether, and the mixed sample was precipitated from solution by adding trimethylamine as a cosolvent.

Pressed pellet samples were made with a hardened steel pellet die in a Carver Laboratory Press. The pellet die, which produced  $3/16$ -in. (0.476 cm) diameter pellets at nominal static pressures of 250–400 atm, was cooled in liquid nitrogen prior to sample introduction in order to prevent decomposition.

When desired, layers of alkali metal were applied to the electrodes of conductivity cells in a helium-filled drybox. The metal was spread on the electrodes with a knife, and care was taken to cover the entire electrode surface. Powder and pellet samples were also loaded in the glovebox when alkali-metal electrodes were used. After application of the metal to the electrodes, the conductivity cell was cooled to  $\sim 200$  K in a cold well in the drybox. The electride samples were transferred into the drybox in Cryotubes that were kept cold in a hollow copper block that had been previously cooled in liquid nitrogen. This procedure prevented decomposition of the samples during evacuation of the air lock. Once inside the drybox, the ampule was broken open and the sample was placed in the conductivity cell, which was then quickly assembled and removed from the box.

Two methods of sample temperature control were used for the different conductivity experiments. For variable-temperature experiments, the conductivity cell was placed in a "soft" 30-L liquid nitrogen dewar that had been precooled with liquid nitrogen. The dewar was then allowed to warm to room temperature while the conductivity experiment was performed. Warm nitrogen gas was circulated through the dewar to increase the rate at which the dewar warmed. The flow rate of the nitrogen gas could be adjusted to warm the dewar from 77 K to room temperature in 12–48 h. The cryostat used for constant-temperature experiments consisted of a 2-in.-diameter glass tube closed on the bottom end and inserted into a partially filled 30-L liquid nitrogen dewar. The sample temperature was controlled by its height in the tube and could be stabilized to within  $\pm 0.1$  K for periods of more than 24 h.

The cell used for dc conductivity measurements has been described in detail elsewhere.<sup>1,11</sup> It consists of two stainless steel rods as electrodes and a glass tube as the sample chamber. The lower electrode is fixed, and samples are compressed against it by the spring-loaded top electrode. In its original design, the cell was unshielded. For the present work, both electrodes were electrically insulated from the cell body by Teflon spacers. The cell body was then connected to the shield of the coaxial leads used in the conductivity measurements. This arrangement kept background currents below 1 pA and allowed resistances up to  $10^{13}$   $\Omega$  to be measured.

For impedance spectroscopy experiments, the simpler and more compact cell, shown in Figure 1a, was used. A top spring-loaded electrode compressed the sample against a bottom stainless steel plate electrode. The cell has a brass body that is electrically connected to the bottom electrode. The sample chamber is a Delrin cylinder with a  $1/16$ -in.-diameter hole into which a pressed pellet or powder could be introduced.

The four-probe ac conductivity cell for measurements on pellets is shown diagrammatically in Figure 1b. The sample was inserted into a  $3/16$ -in.-diameter Delrin cup. Electrical connections to the pellet were made through four "pogo stick" type connections<sup>12</sup> arranged in a square configuration to contact the sample near its periphery. The "pogo" connections are spring-loaded and set into a Delrin probe holder that can slide up and down in two slots cut into the cell body. When the screw ring is rotated, it forces the probe holder and probes against the pellet. The tips of the probes were usually coated with a small amount of alkali metal

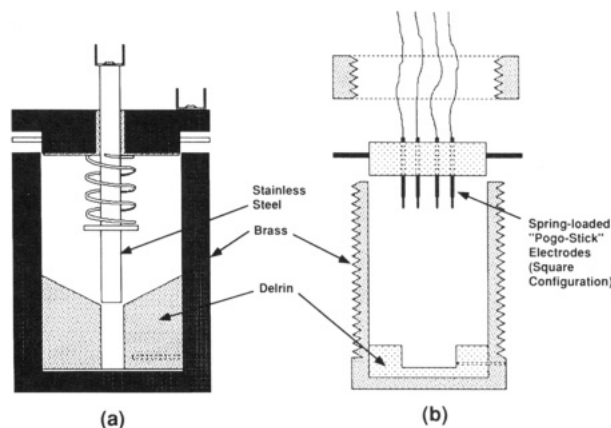


**Figure 1.** (a) Packed powder and pellet conductivity cell for impedance spectroscopy. The  $3/16$ -in.-diameter cylindrical stainless steel electrode is spring-loaded to compress the powder under 20–40 atm. (b) Diagrammatic representation of four-probe conductivity cell for use with compressed pellets. The four "pogo-stick" electrodes are arranged in a square configuration to contact the  $3/16$ -in.-diameter pellet 0.7 mm from the edge.

to ensure good electrical contact to the sample pellet, to prevent decomposition at the electrodes, and to minimize the Schottky barrier between the electrode and the sample (discussed below).

All electrical instrumentation was interfaced through IEEE-488 buses to an IBM PC/XT computer used for instrument control and data acquisition. Dc conductivity was measured with a Keithley Model 617 programmable electrometer. For variable-temperature measurements the electrometer was used as either a sensitive ohmmeter or, more often, as a programmable voltage source and ammeter. When used in the latter mode, it was programmed to apply rectangular voltage pulses of alternate polarity to the sample in order to minimize polarization effects. Temperature measurements for these experiments were made via a Lakeshore Cryotronics Model CGR-1-100 four-probe carbon-glass thermometer and a Keithley Model 580 microohmmeter. Voltage-current measurements for Ohm's law experiments used the Keithley 617 electrometer in the voltage source/ammeter mode. Typically, each voltage was applied for 10 s. The current through the sample at each voltage was measured at approximately a 3-Hz rate. The source voltage was disconnected between each set of readings for 30–60 s in those cases that showed a time-dependent signal.

Impedance spectroscopy<sup>13</sup> (IS) and ac conductivity experiments utilized a Hewlett-Packard low-frequency impedance analyzer. The instrument can apply voltages from 5 to 1100 mV in the frequency range of 5 Hz to 13 MHz. For IS experiments, the magnitude of the impedance vector,  $|Z|$ , and its phase shift,  $\Phi$ , were measured. The data at each frequency were transformed into the complex impedance plane by using the equations

$$\text{Re}(Z) = |Z| \cos \Phi \quad \text{Im}(Z) = |Z| \sin \Phi \quad (1)$$

where  $\text{Re}(Z)$  and  $\text{Im}(Z)$  are the real and imaginary parts of the impedance, respectively.

## Results and Discussion

The electrides  $\text{K}^+(\text{C}222)\text{e}^-$ ,  $\text{Cs}^+(15\text{C}5)_2\text{e}^-$ , and  $\text{Cs}^+(18\text{C}6)_2\text{e}^-$  were chosen for this study because their crystal structures are known. The structures of electrides and alkalides are usually dominated by the nature of the cation packing. In  $\text{K}^+(\text{C}222)\text{e}^-$ , cation packing leaves large vacancies ( $\sim 4 \times 6 \times 12$  Å) in the structure in which pairs of electrons are presumably trapped.<sup>14,15</sup> The cavities are connected in one crystal direction by short open channels

(13) MacDonald, J. R. *Impedance Spectroscopy*; Wiley-Interscience: New York, 1987.

(14) Huang, R. H.; Faber, M. K.; Moeggenborg, K. J.; Ward, D. L.; Dye, J. L. *Nature* 1988, 331, 599–601.

(15) Ward, D. L.; Huang, R. H.; Dye, J. L. *Acta Crystallogr.* 1988, C44, 1374–1376.

(11) Yemen, M. R. Ph.D. Dissertation, Michigan State University, 1982.

(12) Augat/Pylon Co., Inc., P.O. Box 2510, Attleboro Falls, MA 02763.

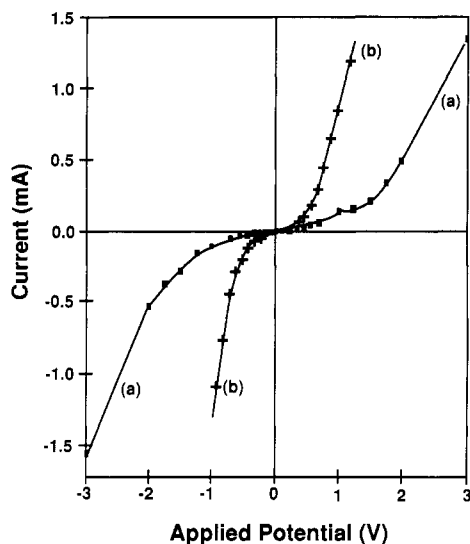


**Figure 2.**  $I$ - $V$  curves for  $K^+(C_{222})e^-$  packed powders at 85 K (a) between stainless steel electrodes and (b) between one stainless steel electrode and one electrode coated with potassium metal.

( $\sim 4$ -Å diameter) and in another direction by somewhat more constricted channels.<sup>14</sup> Temperature-dependent magnetic susceptibility data show that the electrons of  $K^+(C_{222})e^-$  have a spin-paired (singlet) ground state, but with a triplet (or dissociated) state about 0.05 eV above the ground state.<sup>14</sup> By contrast, the structures of  $Cs^+(15C_5)_2e^-$  and  $Cs^+(18C_6)_2e^-$  have smaller anionic cavities ( $\sim 4.7$  Å in diameter and  $\sim 4 \times 4 \times 6$  Å, respectively) that are connected by rather constricted channels.<sup>16,17</sup> In both of these compounds, magnetic susceptibility measurements indicate that, at least above about 30 K, the electrons are predominantly unpaired and exist as isolated trapped electrons.<sup>16,18</sup> Because of their different structures, it was expected that these three electrides would exhibit different electrical properties. Temperature-dependent powder X-ray diffraction studies<sup>19</sup> and alkali-metal NMR spectra<sup>18,20</sup> both indicate that considerable motion of the complexant occurs above about 200 K in alkaliides and electrides and that the process is reversible. This could affect both electronic and ionic conductivities.

**$K^+(C_{222})e^-$ .** Early interest in the electrical properties of  $K^+(C_{222})e^-$  was sparked by the optical spectra of solvent-free films of the compound. These films show broad, plasmon-like absorptions throughout the visible and near-IR regions similar to those observed in metallic solutions of alkali metals in ammonia.<sup>21</sup> EPR measurements, particularly the pronounced effect on the cavity "Q" of a sample that contained only a barely visible particle, indicated high microwave conductivity, as did the Dysonian EPR line shape.<sup>22</sup> This agreed with earlier qualitative microwave conductivity measurements on powders prepared by solvent evaporation,<sup>23</sup> which showed behavior similar to that of powdered metals. The need for large cooled samples and the unavailability of specialized ap-

(16) Dawes, S. B.; Ward, D. L.; Huang, R. H.; Dye, J. L. *J. Am. Chem. Soc.* 1986, 108, 3534-3535.

(17) Ward, D. L.; Huang, R. H.; Kuchenmeister, M. E.; Dye, J. L. *Acta Crystallogr. C* 1990, C46, 1831-1833.

(18) Dawes, S. B.; Eglin, J. L.; Moeggenborg, K. J.; Kim, J.; Dye, J. L. *J. Am. Chem. Soc.* 1991, 113, 1605-1609.

(19) Doueff, S.; Tsai, K.-L.; Dye, J. L. *Inorg. Chem.* 1991, 30, 849-851.

(20) Dawes, S. B.; Ellaboudy, A. S.; Dye, J. L. *J. Am. Chem. Soc.* 1987, 109, 3508-3513.

(21) DaGue, M. G.; Landers, J. S.; Lewis, H. L.; Dye, J. L. *Chem. Phys. Lett* 1979, 66, 169-172.

(22) Faber, M. K. Ph.D. Dissertation, Michigan State University, 1985.

(23) DaGue, M. G. Ph.D. Dissertation, Michigan State University, 1979.

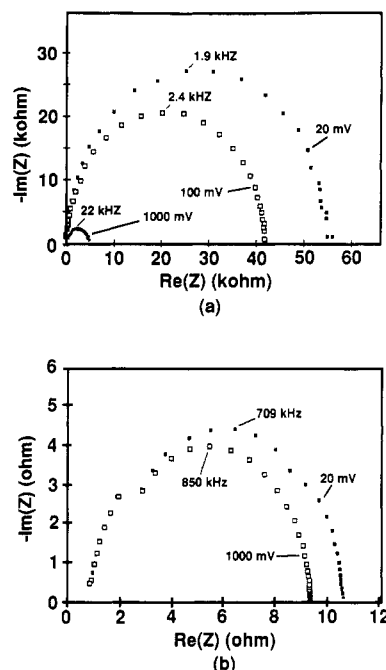


**Figure 3.** Impedance spectroscopy curves at 90 K for  $K^+(C_{222})e^-$  (a) between stainless steel electrodes and (b) between stainless steel electrodes coated with potassium metal. (Note the difference of  $10^3$  in the scale factors.)

paratus for quantitative microwave conductivity measurements prevented further studies of this type. In the present work, preliminary dc conductivity measurements showed semiconductor-like behavior, with an apparent bandgap of only 0.02-0.06 eV but with a higher resistance than anticipated for a material with such a small bandgap. In addition, marked nonohmic behavior was observed for the compound as shown in Figure 2a. Such extreme curvature of an  $I$ - $V$  plot is usually due to grain boundary or electrode contact effects rather than to bulk sample properties.

Impedance spectroscopy experiments on  $K^+(C_{222})e^-$  yielded single voltage-dependent impedance arcs at each voltage for both steel and gold electrodes. Representative spectra are shown in Figure 3a, and it can be seen that the low-frequency intercept decreases by an order of magnitude as the voltage is increased from 20 to 1000 mV. Although both steel and gold electrodes gave voltage-dependent spectra, the impedance arc was  $\sim 2$  orders of magnitude smaller when gold electrodes were used, indicating that an electrode effect is involved. In addition, the arc did not intersect the origin of the complex plane at high frequencies as would be expected for a bulk sample arc.

The electrode-sample impedance could result from either a Schottky barrier or a resistive layer. Schottky barriers are commonly formed when semiconducting samples contact a metallic electrode.<sup>24</sup> In most such contacts, the Fermi levels of the two materials lie at different energies, and charge flows between the materials upon contact until the Fermi levels align. This process causes the formation of a depletion region and a barrier to current flow in the semiconductor. The height of the Schottky barrier depends on the initial offset in the Fermi levels of the two materials. The other possible cause of the high resistance, a decomposed layer at the sample-electrode interface, is common when the sample is easily oxidized. However, only a thin layer, through which electron tun-

(24) Sze, S. M. *Physics of Semiconductor Devices*; Wiley-Interscience: New York, 1981.

neling could occur, would yield pronounced voltage dependence.

When samples of  $\text{K}^+(\text{C222})\text{e}^-$  were placed between two electrodes coated with potassium metal, the observed impedance spectrum was very different. As shown in Figure 3b, the impedance arc still did not pass through the origin but was much smaller and had much less voltage dependence than had been observed with either gold or steel electrodes. The temperature dependence of this arc yielded an apparent bandgap of  $\sim 0.04$  eV. Measurements of two-probe dc resistances between potassium electrodes were not feasible with our apparatus because the low resistance of the sample was masked by the resistances of the leads. When a sample was placed between one steel and one potassium electrode, the sample resistance was about half that between two steel electrodes and the  $I$ - $V$  curves were symmetric about  $V = 0$  but still distinctly curved (Figure 2b).

Two additional possible causes of the effect of potassium electrodes required further study. Since the alkalide  $\text{K}^+(\text{C222})\text{K}^-$  exists, it was possible that potassium metal had reacted with  $\text{K}^+(\text{C222})\text{e}^-$  to form the alkalide, which might be highly conductive. A second possibility was dispersion of potassium metal from the electrodes to form a conductive path.

Proof that the formation of  $\text{K}^+(\text{C222})\text{K}^-$  was not responsible was obtained from impedance spectroscopy studies of this potasside. When steel electrodes were used, its impedance spectrum consisted of two distinct but partially overlapping arcs. The large, low-frequency arc was strongly voltage dependent. When potassium electrodes were used, the higher impedance arc vanished, leaving only a lower impedance arc that was nearly voltage independent. The low-frequency intercept of this arc was  $\sim 10^4$  times larger than that observed for  $\text{K}^+(\text{C222})\text{e}^-$  under the same conditions, showing that  $\text{K}^+(\text{C222})\text{K}^-$  is much less conductive than the electride.

To test for dispersed potassium metal in  $\text{K}^+(\text{C222})\text{e}^-$ , a sample of the compound was placed between potassium electrodes for 24 h. The sample was then separated from the potassium electrodes and placed in a cell between steel electrodes. The behavior and impedance spectrum of this sample were virtually identical with those of samples that had not been exposed to potassium. Thus the effect of potassium electrodes is clearly to greatly reduce the electrode-sample resistance, and we conclude that most of the resistance observed with steel or gold electrodes occurred at the electrodes.

Four-probe ac conductivity studies were performed on pressed pellets of  $\text{K}^+(\text{C222})\text{e}^-$  to minimize electrode contact effects. The electrode tips were coated with potassium to further reduce the contact resistance. To prevent crumbling of the sample, the contacts were placed 0.7 mm in from the perimeter of the pellet. Data were collected over the temperature range 85–230 K by scanning both up and down in temperature. The data shown in Figure 4 yield two linear regions that intersect at a temperature of  $\sim 135$  K. The apparent bandgaps are 0.055 eV at lower temperatures and 0.086 eV above 135 K. Two-probe measurements had indicated the presence of such a break, but the experiments had not been carried to high enough temperatures for the complete break to be observed. The change in slope might be caused by a change from doped (extrinsic) conductivity at low temperatures to intrinsic conductivity at higher temperatures. Evidence for unpaired defect electrons in  $\text{K}^+(\text{C222})\text{e}^-$  is the presence of a Curie law "tail" in the magnetic susceptibility at low temperatures.<sup>14</sup> Alternatively, the change in the apparent

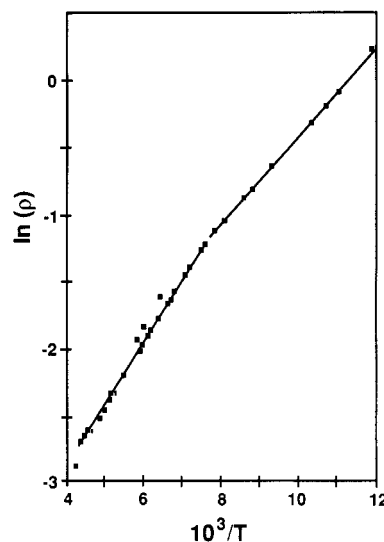


Figure 4. Temperature dependence of the resistivity ( $\Omega$  cm) of a  $\text{K}^+(\text{C222})\text{e}^-$  pellet obtained from four-probe measurements.

bandgap could result from a reversible transition or increased molecular motion.

These results show that  $\text{K}^+(\text{C222})\text{e}^-$  is a highly conductive compound. The high apparent resistivity observed in early conductivity experiments is due to an electrode resistive effect, either from a Schottky barrier or from a resistive layer. The use of potassium metal as an electrode material dramatically reduced the electrode impedance. Since the Fermi level of potassium is much different from that of gold (2.3 as opposed to 5.3 eV), this change in impedance could be interpreted as a lowering of the Schottky barrier by using an electrode material with a Fermi level close to that of the semiconductor sample. Alternatively, potassium metal may react with a resistive layer at the sample-electrode interface to lower the observed impedance. If so, the barrier layer would have to be thin enough to permit electron tunneling in order to give the observed strong voltage dependence of the resistance. With ideal Schottky barriers, diodic behavior would have resulted when samples were placed between one steel and one potassium electrode. The observation of a very nearly symmetric  $I$ - $V$  curve (Figure 2) points toward a resistive layer as the source of the effect. It should be noted, however, that placing a sample between dissimilar electrodes need not result in diodic behavior.<sup>25,26</sup>

The measured resistance of  $\text{K}^+(\text{C222})\text{e}^-$  from four-probe experiments with potassium-coated electrodes includes grain boundary effects and so is probably greater than the intrinsic resistance. The data place an upper limit of 0.2  $\Omega$  cm for the resistivity at 130 K. The measured bandgap of 0.086 eV (in the higher temperature region) is small for a semiconductor. The observed apparent gap is probably not an intrinsic property of the compound but, rather, results from activated transport of electrons across the grain boundaries in the polycrystalline samples. Additional evidence for this interpretation comes from the observed capacitances of the samples. By using the relationship  $\omega CR = 1$  at the maximum in the impedance semicircles,<sup>13</sup> we obtain  $C = 1.6$  nF at all three voltages shown in Figure 3a and  $C = 20$  nF for the data of Figure 3b (with a different sample). These capacitance values are much larger than the geometric capacitance (picofarads) of the sample. Also,

(25) Lipseter, M. P.; Sze, S. M. *Bell Syst. Tech. J.* 1968, 47, 195–208.

(26) Geddes, N. J.; Sambles, J. R.; Parker, W. G.; Couch, N. R.; Jarvis, D. J. *J. Phys. D: Appl. Phys.* 1990, 23, 95–102. (We are indebted to one of the reviewers for pointing out this reference.)

any double-layer capacitance at blocking electrodes would be negligible at potassium-coated electrodes. We conclude that the intrinsic conductivity is greater than that measured because of grain-boundary effects, which are responsible for the large measured capacitance and most of the dc and low-frequency resistance.

Because of the distinctly anisotropic structure of  $\text{K}^+(\text{C}222)\text{e}^-$  (the presence of large, short channels in one direction and smaller channels in a second direction), the plasmon-type absorption spectrum, and the rather high conductivity, it was presumed that this compound might be a low-dimensional metal. If so, however, the metallic nature is obscured by grain-boundary effects. If, on the other hand, the intrinsic conductivity still has an activation energy, it may result from activated (hopping) transport rather than thermal population of a conduction band. Resolution of these questions will require four-probe single-crystal measurements.

$\text{Cs}^+(\text{15C5})_2\text{e}^-$ . The electride  $\text{Cs}^+(\text{15C5})_2\text{e}^-$  contains sandwiched cesium cations and rather isolated trapped electrons.<sup>17,18</sup> Magnetic susceptibility data, <sup>133</sup>Cs NMR experiments, and EPR studies show that these electrons are largely unpaired and do not interact strongly with the cation or with each other, although a transition to an antiferromagnetic state does occur at 4.6 K.<sup>18</sup>

Samples of  $\text{Cs}^+(\text{15C5})_2\text{e}^-$  had dc resistivities that were strongly dependent on the preparation and time. For example, at a temperature of 190 K, three samples had apparent resistivities of  $3.4 \times 10^{10}$ ,  $4.4 \times 10^9$ , and  $2.0 \times 10^7 \Omega \text{ cm}$ , respectively. In all cases, the low-temperature resistivity appeared to be extrinsic with activation energies of 0.19, 0.14, and 0.28 eV, respectively. Plots of  $\ln \rho$  vs  $1/T$  showed steeper slopes above about 235 K with activation energies of about 0.6, 0.5, and 0.8 eV, respectively. The time dependence of the dc resistivity showed that polarization was occurring, and the sample dependence indicated high sensitivity to the composition. The temperature of the break between low and high activation energy regions was not associated with any phase transition detectable by NMR spectroscopy, differential scanning calorimetry (DSC), or magnetic susceptibility. Extrapolation of the low-temperature behavior to  $T = \infty$  yielded limiting resistivities of  $3 \times 10^5$ ,  $3 \times 10^3$ , and  $1 \times 10^2 \Omega \text{ cm}$ , indicative of sample-dependent extrinsic electronic conductivities due to the presence of defect electrons trapped at 0.3–0.5 eV below the conduction band. The presence of such defect electrons in alkaliides and electrides has recently been demonstrated by thermionic emission studies.<sup>27</sup>

To investigate the nature of the conduction process responsible for the high-temperature behavior, impedance spectroscopy as well as dc conductivity measurements were made. IS experiments had to be performed at temperatures above 240 K because of the high impedance of the compound at lower temperatures. The impedance spectrum of  $\text{Cs}^+(\text{15C5})_2\text{e}^-$ , shown in Figure 5, consists of a single, voltage independent arc and a low-frequency spike. Similar spikes are often observed due to blocking electrodes in ionically conductive systems.<sup>13</sup> When the sample was decomposed, the impedance spectra of the decomposed samples also showed blocking behavior and were similar to those of the "live" sample. It should be noted, however, that decomposition produces a soft semiliquid product that is easily squeezed out from between the electrodes.

These results suggested that  $\text{Cs}^+(\text{15C5})_2\text{e}^-$  is an ionic rather than an electronic conductor. The time dependence

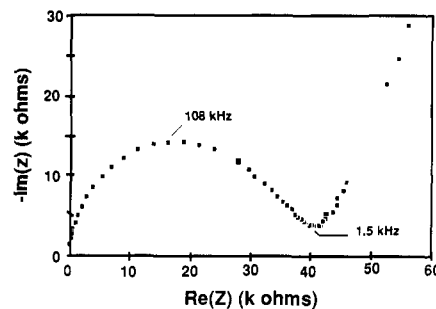
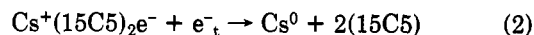


**Figure 5.** Impedance plot at 255 K for a packed-powder sample of  $\text{Cs}^+(\text{15C5})_2\text{e}^-$ . Note the onset of blocking behavior at low frequencies. The dc resistivity between cesium-coated electrodes is 2 orders of magnitude larger than the highest impedance point on this graph.

and voltage dependence of the current in dc experiments support this interpretation. Figure 6a shows these effects when a pressed powder sample was placed between two steel electrodes. The current-voltage curve was strongly nonohmic. At each voltage the current decayed during the 10-s period of measurement and recovered during the "rest period" between measurements. This behavior is expected for ionic conduction because of the formation of a depletion layer and space charge at the positive (blocking) electrode. During the depletion, about  $10^{-5} \text{ C}$  of electricity passed through the cell, which is equivalent to the amount of  $\text{Cs}^+$  in a 30-Å-thick layer of the compound.

When samples of the compound were placed into a cell that had one steel and one cesium electrode, Ohm's law experiments yielded the results shown in Figure 6b. This configuration created an electrochemical cell that produced current even in the absence of an applied voltage. Approximately 100 mV bucking potential was required to zero the current. When voltage was applied to the cell with the cesium electrode positive, the current did not decay with time. With the cesium electrode negative, however, the current decayed with time over the 10-s duration of the measurement but recovered between measurements. No time dependence of the current or curvature of the  $I$ - $V$  plot was observed when both electrodes were coated with cesium metal (Figure 6c).

It appears that  $\text{Cs}^+(\text{15C5})_2\text{e}^-$  is an ionic conductor with an activation energy of about 0.6 eV, that is, however, sample dependent. This is the first evidence of ionic conductivity in an electride. The mechanism of this conductivity might involve in initial release of  $\text{Cs}^+$  from its crown ether cage. The direct transport of  $\text{Cs}^+$  through the crystal seems unlikely since the cation would be reduced to  $\text{Cs}^0$  by the trapped electrons in the system. A possible mechanism involves the release of  $\text{Cs}^+$  from the crown ether cage coupled with its reduction to  $\text{Cs}^0$  by the trapped electron via the reaction

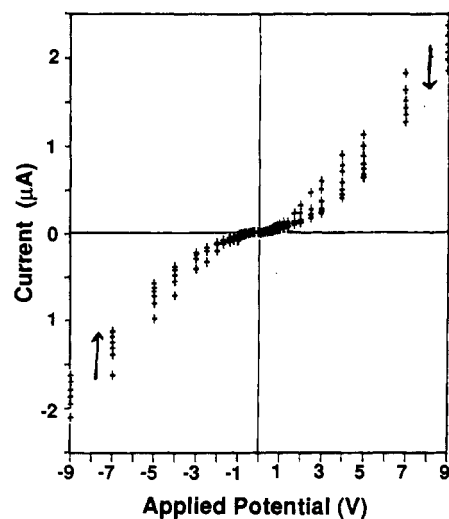


where the  $\text{Cs}^0$  is located in an anionic cavity of the crystal. From this site, the  $\text{Cs}^0$  may be transferred through a channel to the next cavity as  $\text{Cs}^+$ , where it would be reduced back to  $\text{Cs}^0$ , a process that would result in the transport of  $\text{Cs}^+$ .

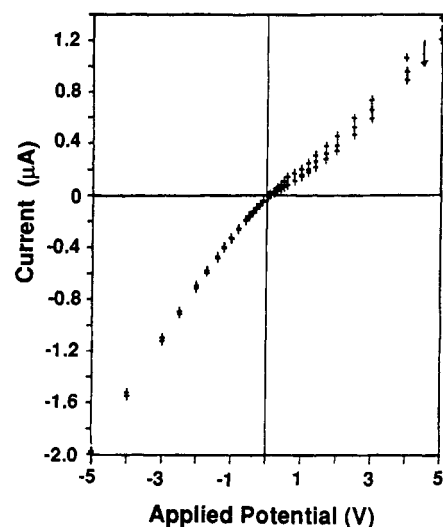
The electrochemical cell behavior of  $\text{Cs}^+(\text{15C5})_2\text{e}^-$  between one steel and one cesium electrode also implies  $\text{Cs}^+$  migration. When the cesium metal electrode is negative,  $\text{Cs}^+$  migrates toward it and away from the steel electrode. This causes the formation of a depletion layer at the steel electrode and the observed time-dependent current. Under reverse bias,  $\text{Cs}^+$  migrates away from the cesium electrode, which acts as a source of  $\text{Cs}^+$  ions. No depletion layer is

(27) Huang, R. H.; Dye, J. L. *Chem. Phys. Lett.* 1990, 166, 133–136.

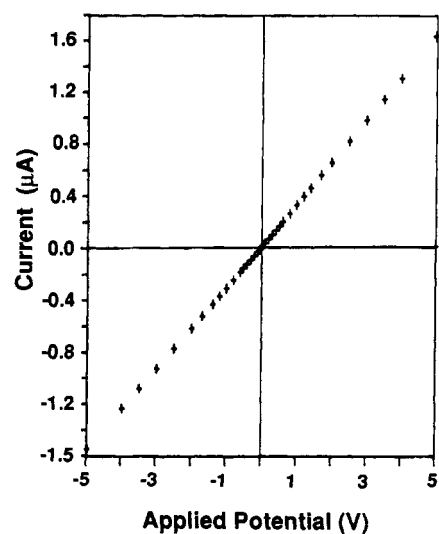




(a)



(b)



(c)

**Figure 6.**  $I$ - $V$  plots for  $\text{Cs}^+(15\text{C}5)_2\text{e}^-$  (a) between stainless steel electrodes at 255 K, (b) with one electrode covered with cesium metal at 247 K, and (c) with both electrodes covered with cesium metal at 246 K. The arrows give the direction of drift of the current over a 10-s period.

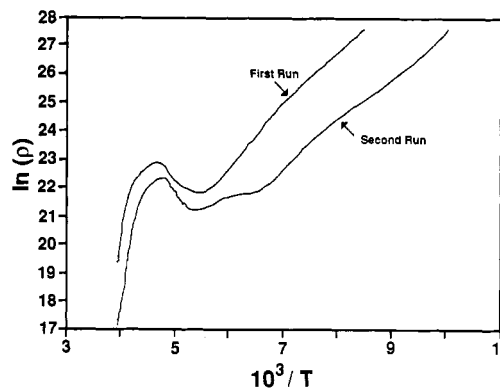
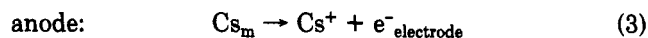


**Figure 7.** Plots of  $\ln \rho$  vs  $10^3/T$  for two pressed-powder samples of  $\text{Cs}^+(18\text{C}6)_2\text{e}^-$  with  $T$  in kelvin and  $\rho$  in  $\Omega \text{ cm}$ . The increase in resistivity between about 180 and 210 K probably results from the same phenomenon that affects the  $^{133}\text{Cs}$  NMR spectrum in this temperature range.<sup>20</sup>

formed, and the current is not time dependent. The process is spontaneous in this direction and results in a net current even at zero applied voltage. One possible set of electrode reactions is



when cesium is present and



when there is no cesium on the electrode, and



When cesium is present on only one electrode, reaction 3 and the reverse of reaction 4 produce an electrochemical potential. It is not possible to predict the potential for this cell reaction, both because the state of  $\text{Cs}^+$  in the solid is unknown when there is no free crown ether and because the state into which electrons are injected at the other electrode is unknown. When both electrodes are coated with cesium, the behavior is strictly ohmic.

$\text{Cs}^+(18\text{C}6)_2\text{e}^-$ . The electride  $\text{Cs}^+(18\text{C}6)_2\text{e}^-$  contains anionic cavities of diameter  $\sim 4 \text{ \AA}$  and length  $\sim 6 \text{ \AA}$ , interconnected by narrow channels.<sup>16</sup> Optical spectra of thin films<sup>7</sup> indicated that the electrons are localized in traps of depth  $> 0.5 \text{ eV}$ . Previous pressed powder conductivity experiments<sup>7</sup> suggested that  $\text{Cs}^+(18\text{C}6)_2\text{e}^-$  is an intrinsic semiconductor with a bandgap of 0.9 eV, but, as described below, this conclusion was incorrect.

Attempts to perform IS studies of ceside-free samples of  $\text{Cs}^+(18\text{C}6)_2\text{e}^-$  were unsuccessful because the impedance was too high for the available instrumentation at any temperature below the decomposition temperature of the compound. The dc conductivities of two samples from different syntheses were drastically different from that obtained previously as shown in Figures 7 and 8. The low-temperature behavior ( $T < 170 \text{ K}$ ) is very similar to that of  $\text{Cs}^+(15\text{C}5)_2\text{e}^-$ , which was attributed to defect electron conductivity. Both compounds have activation energies of  $\sim 0.2 \text{ eV}$  at low temperatures. Above 170 K, the resistance of  $\text{Cs}^+(18\text{C}6)_2\text{e}^-$  first increases and then decreases markedly with increasing temperature. The high-temperature region shows considerable curvature of the  $\ln \rho$  vs  $1/T$  plot (Figure 7) but corresponds to an activation energy of about 1.1 eV.

The increase in the sample resistance with increasing temperature above the crossover temperature is unusual but reproducible. It may be related to the change in the  $^{133}\text{Cs}$  NMR signal over the same temperature range.<sup>20</sup>  $\text{Cs}^+(18\text{C}6)_2\text{e}^-$  shows a gradual reversible change of the

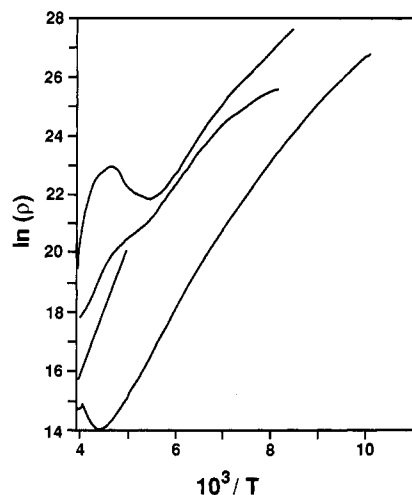


**Figure 8.** Effect of cesium addition to  $\text{Cs}^+(\text{18C6})_2\text{e}^-$  on the temperature dependence of the resistivity. From top to bottom: (1) stoichiometric  $\text{Cs}^+(\text{18C6})_2\text{e}^-$ ; (2) sample with a slight excess of cesium; (3) previous results;<sup>7,8</sup> (4)  $\text{Cs}^+(\text{18C6})_2\text{Cs}^-$ .

NMR signal with temperature that involves the growth of a second  $^{133}\text{Cs}$  peak as the temperature is increased, coupled with the gradual decrease of the low-temperature peak. Evidently, the process responsible also causes an increase in resistivity.

The  $I$ - $V$  data for  $\text{Cs}^+(\text{18C6})_2\text{e}^-$  in the high-temperature region showed curvature but no time dependence of the current. The lack of time dependence is not unexpected in view of the small currents in these experiments (about 3 orders of magnitude below those observed with  $\text{Cs}^+(\text{15C5})_2\text{e}^-$ ). A sample of  $\text{Cs}^+(\text{18C6})_2\text{e}^-$  between a steel electrode and a cesium electrode yielded an electrochemical cell with a potential of 0.6 V. A sample placed between two cesium electrodes gave an Ohm's law plot through the origin with only slight curvature.

These results indicate the presence of ionic conductivity in  $\text{Cs}^+(\text{18C6})_2\text{e}^-$ , in disagreement with the previous work.<sup>7</sup> Further studies were carried out to see whether differences in the synthesis methods could account for the discrepancy. In the previous work, stoichiometric amounts of cesium and crown ether were used in the synthesis, which may have led to contamination by  $\text{Cs}^-$ , although not in high enough concentrations to be observed by  $^{133}\text{Cs}$  NMR. There was no reason at the time to believe that traces of  $\text{Cs}^-$  would affect the electronic conductivity of  $\text{Cs}^+(\text{18C6})_2\text{e}^-$ .

Samples of  $\text{Cs}^+(\text{18C6})_2\text{e}^-$  that contained some ceside were prepared via the two methods described previously. Method A followed the method of synthesis that had been used for the previous work,<sup>7</sup> and method B involved the intentional addition of ceside to an electride sample. It was not possible to determine visually whether phase separation of the product had occurred as a result of the presence of excess cesium since both the alkalide and the electride are dark in color. The conductivities of both samples were similar. No time dependence of the current was observed in dc conductivity experiments, and no electrochemical cell behavior was observed when the samples were placed between one steel and one cesium electrode. Samples of the "doped" electride exhibited mark-

edly increased conductivities compared with the "pure" electride samples (Figure 8). No pronounced break in the conductivity as seen with pure samples was observed for the doped samples. Samples of the ceside,  $\text{Cs}^+(\text{18C6})_2\text{Cs}^-$ , also showed higher conductivity and semiconductor behavior below the decomposition temperature as seen in Figure 8. When a sample of the electride was doped with small amounts of sodide, the results were very different. The dc conductivity up to the decomposition temperature was similar to that of the pure electride. That is, contamination by  $\text{Na}^-$ , which can fit into the cavity,<sup>16,28</sup> does not increase the conductivity as does contamination by the very large  $\text{Cs}^-$  ion.

$\text{Cs}^+(\text{18C6})_2\text{e}^-$  appears to be an ionic conductor with an activation energy of about 1.1 eV. The conduction mechanism is probably closely related to that of  $\text{Cs}^+(\text{15C5})_2\text{e}^-$ . If a large part of the activation energy involves release of  $\text{Cs}^+$  from its crown ether cage, the observed relation between the activation energies of these two electrides can be understood. Since the cation complex of  $\text{Cs}^+(\text{18C6})_2\text{e}^-$  is more tightly bound than that of  $\text{Cs}^+(\text{15C5})_2\text{e}^-$ , the increased activation energy of conductivity in the former may reflect the increased stability of this complex.

The present results have shown that the semiconductor behavior seen previously<sup>7</sup> in samples of  $\text{Cs}^+(\text{18C6})_2\text{e}^-$  was probably the result of ceside doping of the compound. Intentional doping of electride samples with cesium resulted in increased electronic conductivity of the compound, which masked the effects of ionic conductivity. When sodium was used as the dopant, the conductivity was virtually the same as that of the pure electride. The reason for the observed difference may be the differences in sizes of the dopant anions. The cesium anion ( $\sim 7.0$  Å in diameter) is too large to fit easily into the anionic cavities of  $\text{Cs}^+(\text{18C6})_2\text{e}^-$ . As a result, one of the 6s electrons of  $\text{Cs}^-$  may go into a Rydberg-type orbital around the smaller Cs atom from which it can readily be excited into the conduction band of  $\text{Cs}^+(\text{18C6})_2\text{e}^-$ . The absence of increased conductivity in the sodium-doped system can also be explained. The diameter of the sodium anion is  $\sim 5.0$  Å, approximately the same size as the anionic sites in  $\text{Cs}^+(\text{18C6})_2\text{e}^-$ , and so would fit more easily into the structure.

These conductivity results with  $\text{Cs}^+(\text{15C5})_2\text{e}^-$  and  $\text{Cs}^+(\text{18C6})_2\text{e}^-$  demonstrate the importance of high-purity samples in conductivity experiments. They also suggest the need to reexamine the conductivity properties of alkalides and electrides that have been measured in the past. As seen for  $\text{Cs}^+(\text{18C6})_2\text{e}^-$ , the results of such experiments depend dramatically upon the synthesis methods employed. In particular, ionic conductivity may be much more common in alkalides and electrides than was previously thought.

**Acknowledgment.** We are grateful for support of this research from the U.S. National Science Foundation Solid-State Chemistry Grant No. DMR 87-17763 and the Michigan State University Center for Fundamental Materials Research.

(28) Dawes, S. B.; Ward, D. L.; Fussa-Rydel, O.; Huang, R. H.; Dye, J. L. *Inorg. Chem.* 1989, 28, 2132-2136.